Zihui Wang[1], Qinfen Lu[1], Yunyue Ye[1], Kaiyuan Lu[2], Youtong Fang[1]

1. Zhejiang University, China 2.Aalborg University, Denmark

Investigation of PMSM Back-EMF using Sensorless Control with Parameter Variations and Measurement Errors

Abstract. *To achieve better performance of sensorless control of PMSM, a precise and stable estimation of rotor position and speed is required. Several parameter uncertainties and variable measurement errors may lead to estimation error, such as resistance and inductance variations due to temperature and flux saturation, current and voltage errors due to measurement uncertainties, and signal delay caused by hardware. This paper reveals some inherent principles for the performance of the back-EMF based sensorless algorithm embedded in a surface mounted PMSM system adapting vector control strategy, gives mathematical analysis and experimental results to support the principles, and quantify the effects of each. It may be the guidance for designers to minify the estimation error and make proper on-line parameter estimations.*

Streszczenie. *Do otrzymania dobrych parametrów sterowania silnikiem PMSM niezbędne jest określanie precyzyjnie pozycji wirnika i prędkości. Zmiany rezystancji i indukcyjności z temperaturą oraz zmiany strumienia nasycenia mogą powodować błędy estymacji. W artykule przedstawiono wbudowany algorytm bazujący na metodzie back-EMF wykorzystujący strategię adaptacyjnego sterowania wektorowego. (**Badania parametrów sterowania silnikiem PMSM z wykorzystaniem metody back-EMF z uwzględnieniem zmienności parametrów i błędów pomiarowych**)*

Keywords: Back-EMF, PMSM, sensorless control, parameter variations, measurement errors
Słowa kluczowe: back EMF, silnik PMSM, sterowanie bezczujnikowe

Introduction

Instead of using mechanical position sensor, sensorless technic of permanent magnet synchronous machines (PMSMs) is a hot issue which focus on calculating rotor position or speed using electrical information measured. The Back-EMF based sensorless algorithm is mature enough and has already been combined with vector control strategy in industrial applications. The performance of the Back-EMF based sensorless vector control is mainly determined by the sensorless algorithms with respect to the position and speed estimation. Take some factors as an example, the system efficiency will be reduced by erroneous field orientation if the estimated rotor position is not quite aligned with the actual position. Furthermore, non-convergent estimation results will cause speed and torque oscillation and the system might be unstable.

Recently, the back-EMF based methods are only intended to be operated in medium to high speed range. A general point of view is that the back-EMF based sensorless algorithm suffers from the small amplitude of back-EMF signals at low speed [1]-[2]. The signal uncertainty may cause system unstable or even operation failure. On the other hand, some parameter uncertainties and variable measurement errors affect the estimation accuracy. For example, the resistance variations and inverter irregularities contribute to the estimation error at low speed [3]-[5]. However, at high speed some other parameter uncertainties contribute dominant estimation error, such as the inductance saturation effects [6] and the PWM signals delay caused by control unit of the inverter [7].

The influence of the current measurement errors and inverter irregularities on estimated rotor position at low speed was studied in [4]. It showed that the voltage drops in electronic components of the inverter and the dc source voltage measurement error affect the control performance. The errors caused by current sensors contribute a constant disturbance and harmonics of one and two to the estimation error. A compensation method for resistance error was also proposed in [4]. More articles analyzed the estimation error with respect to some other error sources as [8]-[9]. However, those studies were mainly focus on the accuracy and stability at low speed, which was not a conventional operation state for most applications. For all speed range, the discussion of inherent laws of Back-EMF based sensorless estimation error was not sufficient or detailed enough.

This work theoretically analyzes the estimation errors caused by parameter and variable variations, and then find error sources and provide a revision guideline for the estimation result. Section II gives a brief introduction of the Back-EMF sensorless algorithm. Section III investigates the main factors affecting sensorless performance. Section IV shows how those factors disturb parameters or variables and how they degrade the sensorless performance, and quantify the effects of each. Finally, conclusions are presented in Section V.

Description of back-emf based sensorless algorithm

The electromagnetic principle of the PMSM may be illustrated as a voltage vector equation (1) and a phasor diagram as Fig.1. The conventional back-EMF sensorless algorithm is based on the back-EMF orientation in stator, as described in (2)-(5) in stationary *αβ* coordinates:

(1) $$\vec{U} = R\vec{I} + j\omega L\vec{I} + \vec{E}$$

(2) $$u_\alpha = R_s i_\alpha + \frac{d}{dt}(L_s i_\alpha + \psi_{pm}\cos\theta_r)$$

(3) $$u_\beta = R_s i_\beta + \frac{d}{dt}(L_s i_\beta + \psi_{pm}\sin\theta_r)$$

(4) $$\psi_{\alpha\beta} = \int (u_{\alpha\beta} - R_s i_{\alpha\beta})dt$$

(5) $$\theta_r = \tan\frac{\psi_\beta - L_s i_\beta}{\psi_\alpha - L_s i_\alpha}$$

where, *Ψ, U* and *I* are the stator flux linkage, phase voltage and phase current. Suffix *α* and *β* stands for their corresponding *αβ* components. R_s is the stator phase resistance, L_s is the average *dq* inductance. Ψ_{pm} is the permanent magnetic flux. θ_r is the rotor angular position in electrical radians.

In order to operate the back-EMF sensorless algorithm, the parameters need to be known are the stator resistance and the stator inductance, the variables need to be measured are just stator phase currents. Since the stator voltages are obtained by PWM signal reconstruction from dc-link voltage and can be adjusted automatically by current loops [10], voltage measurement is not necessary. In (5), the permanent magnetic flux is reduced while dividing α back-EMF component from β component, so the PM flux variation due to temperature could be ignored. Therefore, only two motor parameters and one measured variable are necessary for rotor position estimation. The algorithm has a very good robustness from medium to high speed range.

Parameters error influence on the algorithm

To make the position estimation simple, motor parameters are usually considered as constants and do not vary with the changes of speed and load. However, some parameters are not kept constant in actual operation. With respect to the true value of the PMSM parameters, e.g. for the winding resistance and inductance in the stator, the values without error are noted as R_s and L_s, whilst the nominal values with error included are noted as $\hat{R}_s$ and $\hat{L}_s$. So the errors in the parameter nominal values with respect to the true values are defined as follows:

(6)
$$\left.\begin{aligned}\Delta R_s &= \hat{R}_s - R_s \\ \Delta L_s &= \hat{L}_s - L_s\end{aligned}\right\}$$

Considering measurement uncertainties, the case is similar to the variables, e.g. the current might be mistakenly sampled by sensors or the nominal stator voltage might be over reconstructed due to IGBT dead-time loss. The variable errors in the nominal values ($\hat{u}, \hat{i}$) with respect to the true values (u, i) are defined as follows:

(7)
$$\left.\begin{aligned}\Delta u &= \hat{u} - u \\ \Delta i &= \hat{i} - i\end{aligned}\right\}$$

According to the phasor principle of PMSM in Fig.1, it can be deduced that the back-EMF vector $\vec{E}$, which contains the rotor position information, is inherently constrained by the true value of the motor parameters and measured variables in (1). But in estimation algorithm, the nominal values are substituted into (4)(5), which will slightly differ from the true values, as described in (8). Therefore, the error between nominal and true values accounts for the estimated position error θerr , as figured in Fig.2.

(8)
$$\hat{\theta}_r = \tan^{-1}\frac{\hat{\psi}_\beta - \hat{L}_s\hat{i}_\beta}{\hat{\psi}_\alpha - \hat{L}_s\hat{i}_\alpha}$$

(9)
$$\theta_{err} = \hat{\theta}_r - \theta_r$$

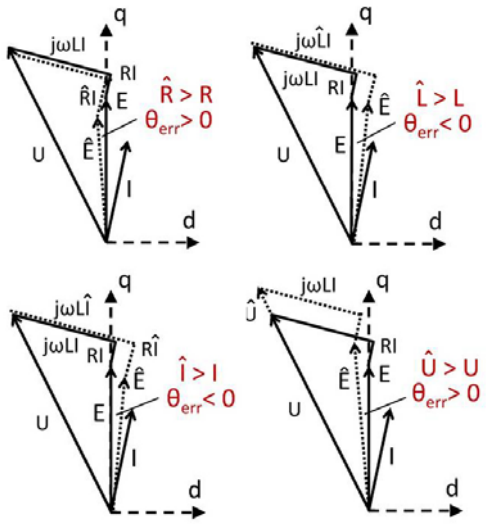

Fig. 2 Estimation error due to parameter and variable variations (a)Error due to erroneous resistance; (b)Error due to erroneous inductance; (c)Error due to erroneous current; (d)Error due to erroneous voltage

From Fig. 2 (a) to (d), it is clear to find difference between the estimated position and the true position, figured as the back-EMF vector $\vec{E}$ (which is 90 degrees ahead of the rotor position). If nominal values of resistance, inductance and current are larger than their true values, the estimated position lags the real rotor position, and vice versa. If the reconstructed voltage is larger than its true value which is actually applied to phase terminals, the estimated rotor position leads the real position, and vice versa. The conclusions:

(1) The estimated rotor position error are negative correlated to errors of stator resistance, stator inductance and measured currents.

(2)The estimated rotor position error is positive correlated to the error of stator voltage.

System error analysis

The back-EMF based sensorless estimation works well from medium to high speed range. However, if the parameters and variables have unexpected errors, the estimated rotor position may vary from its true value. The estimated error may lead to erroneous current decoupling in field oriented control, and make system unstable or cause efficiency loss.

The experimental platform consists of a surface mounted PMSM, a DC motor as the load, an eZdsp^{TM}-F28335 controller, a Danfoss FC302 Series inverter, a 2048-pulses incremental encoder used for validating the actual rotor position, and the CCS3.3 platform used for observing system parameters and variables.

Table 1. Motor parameters

Type: Surface Mounted PMSM			
Rated power	0.47 kW	Stator resistance	2.35Ω
Rated current	2.9 A	d-axis inductance	13.4 mH
Rated speed	2850 rpm	q-axis inductance	15.4 mH
PM flux	0.132Wb	Pole pairs	2

A. Error with respect to resistance variation

One comment for the source with respect to rotor position estimation error at low speed range is considered as the stator resistance variation, as supported by [3]. The resistance varies with the change of the temperature and the excitation current frequency. When running at low speed, usually low load as well, the stator current is relatively small and the thermal effect is not obvious. As a result, it causes an insignificant error as the resistance dose not vary a lot at low speed range. On the other hand, while the motor is running at high speed range or with heavy load, the voltage drop on the resistance is comparatively a neglectable part among the total terminal voltage, as illustrated in Fig. 2(a). The experiment result in Fig.3 also gives a support that the resistance variation with respect to position estimation error could be safely neglected at rated speed with load when its nominal value changes from 100% to 300% of the true value.

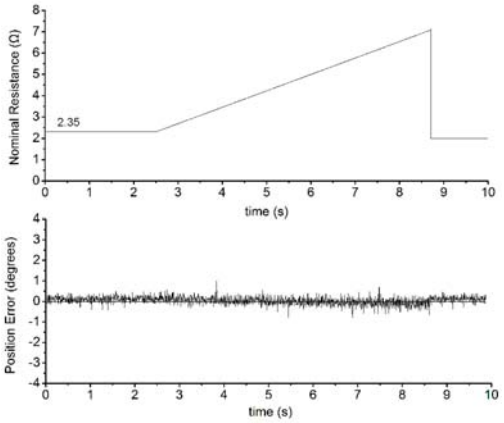

Fig.3 Estimation error due to resistance variation

B. Error with respect to inductance variation

It is well reported that the inductance is sensitive to magnetic saturation [5]-[8],[11]. With the stator current increasing, the inductances may decrease due to magnetic saturation in *d*-axis and *q*-axis. For PMSM, the permanent magnets provide a d-axis magnetic flux which makes the *d*-axis more easily to be saturated than *q*-axis, compared in Fig.4. Especially in conventional i_d=0 vector control strategy, the *d*-axis current is kept to be zero, whilst the *q*-axis current is dependant on the load and changes frequently. Therefore, the *q*-axis inductance varies much faster than *d*-axis inductance, which may happen at different current ranges and heavily depends on the machine design [11]. In high speed or heavy load operation, the q-axis inductance variation is enlarged by the *q*-axis current, and it contributes more significant error to the estimation result. However, for the same amplitude of d- and q-axes current excitations, the d-axis inductance varies more significantly than *q*-axis inductance, so that it contributes more significant error to the estimation result.

Fig.5 shows an inductance changing test (L_s from 80% to 120% of its nominal value), and the estimated position error varies within ±3 electrical degrees. Normally, the part of the voltage drop with respect to inductance and current ($\omega I \Delta Ls$) is much smaller than the dominant back-EMF (E) as in (1), so the erroneous effect by inductance variation is relatively small.

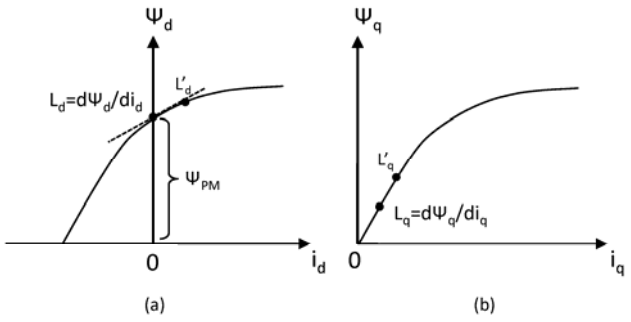

Fig.4 *dq*-inductances variation due to current and flux saturation in *dq*-axes. (a) L_d, (b)L_q

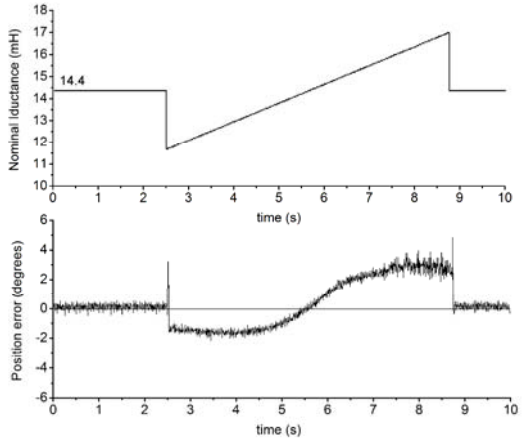

Fig.5 Estimation error due to inductance variation

C. Error with respect to current variation

In steady state, the phase currents are sinusoidal with the angular frequency of ω ,the error caused by measurement differs from its true value by a gain error e_{gain} and an offset e_{off} :

$$\Delta i = \hat{i} - i = e_{gain} \cdot \sin \omega t + e_{off} \tag{10}$$

Detailed analysis was proposed in [4], that the estimation error regarding current measurement error might be decomposed into three components: a constant shift, a component at frequency ω and a component at frequency 2ω , tuned by the gain error and offset value.

Since the current error is negative correlated to the estimation error as mentioned in Part Ⅱ , it could be deduced that the estimation error contains those three components as well, at frequency of 0, ω and 2ω , demonstrated in Fig.11.

D. Error with respect to voltage loss by dead-time effect

The inverter nonlinearity caused by the dead-time effect on switches commutation is one reason for voltage loss. Dead time is needed to prevent shoot-through during the commutation. The dead time, added to the IGBT's turn-on and turn-off times, introduces a current dependant magnitude and phase error in the output voltage. That means the actual voltage *u* on 3-phase terminals are smaller than their nominal value $\hat{u}$ commanded by control unit [12], as shown in Fig.6.

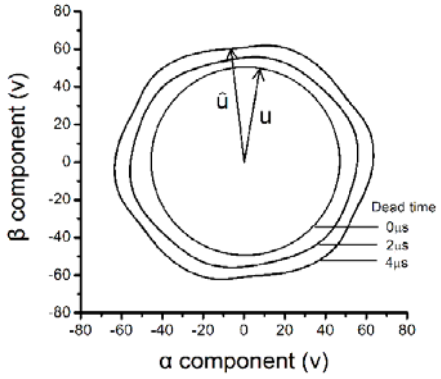

Fig.6 Distorted nominal stator voltage caused by dead-time effect in *αβ* reference frame

When in vector control strategy, the command terminal voltage vector is governed by current-closed loop. As the current-closed loop constrains the stator current to be sinusoidal, the 3-phase terminal voltages are forced to be sinusoidal as well, as the inside circle illustrated in Fig.5. Superimposing the voltage loss, the nominal voltages should be non-sinusoidal [13]. The compensated voltages caused by dead-time effect are shown as the gap area between the inside circle and the outside quasi-circles in Fig.5. The nominal voltage vector (outer quasi-circle) contains a six-order disturbance, which is the reflection of six zero-crossing clamping points for 3-phase currents in each fundamental period. As a result, the estimation position error also contains a component at frequency of 6ω , demonstrated in Fig.11.

E. Error with respect to PWM signal delay

When observing the estimation error according to (9) in experiment, a significant dc offset is revealed. It accounts for a dominant value of the error, which is exactly proportional to the speed. Further research reveals that the offset is also proportional to the PWM switching period (inverse proportional to switching frequency), which can be described as:

$$\theta_{err\_dc} = k \cdot \omega \cdot T_s \tag{11}$$

where *K* is a constant coefficient, ω is the fundamental speed, T_s is the switching period of PWM signals.

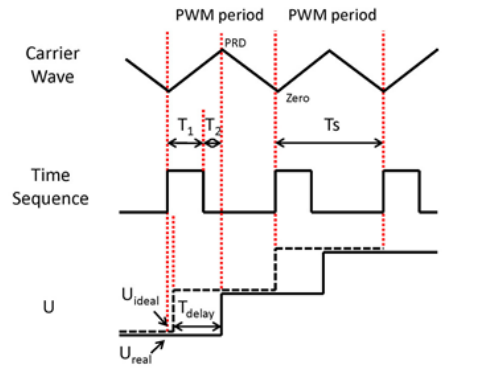

(a) Voltage data update at CTR=PRD or CTR=both PRD&Zero

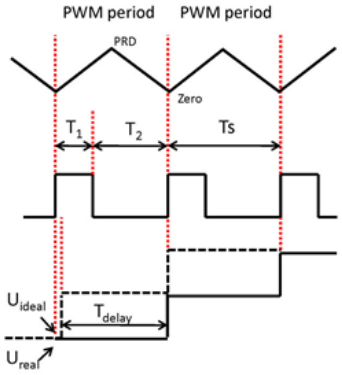

(b) Voltage data update at CTR=Zero

Fig.7 Voltage delay due to "shadowed" PWM output

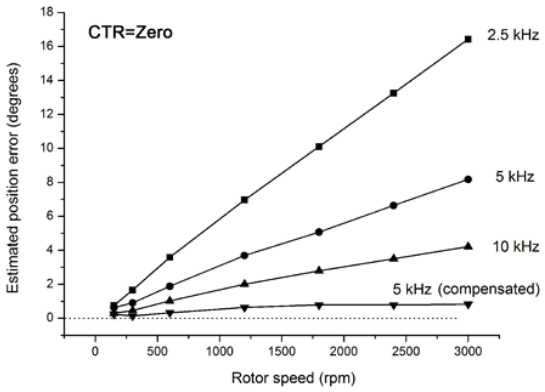

Fig.8 Estimation error caused by PWM signal delay with different speed

This significant error is associated with the signals output delay in DSP PWM module. The PWM signals are generated by comparison between the values in the Time-based Counter and the Compare Registers. In each PWM period, the expected compare values are stored in the Compare Registers which will be output after a short period of time, so called "Shadow Mode". This prevents corruption or spurious operation due to the register being asynchronously modified by software [14]. When shadowing is used, compare value updates only at strategic points. The strategic points could be set at two different moments:

- The time when Time-base Counter value (CTR) equals to period value (PRD): CTR=PRD;

The time when Time-base Counter value equals to zero: CTR=Zero;

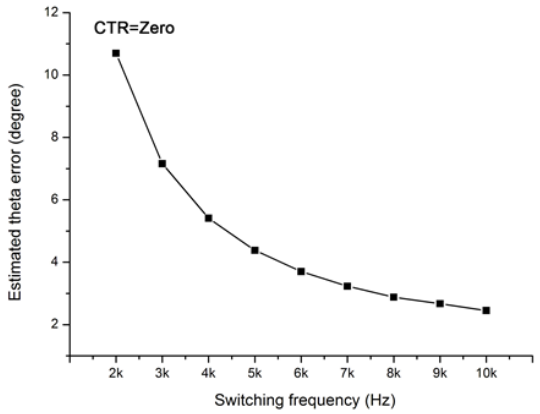

Fig.9 Estimation error caused by PWM signal delay with different PWM frequencies

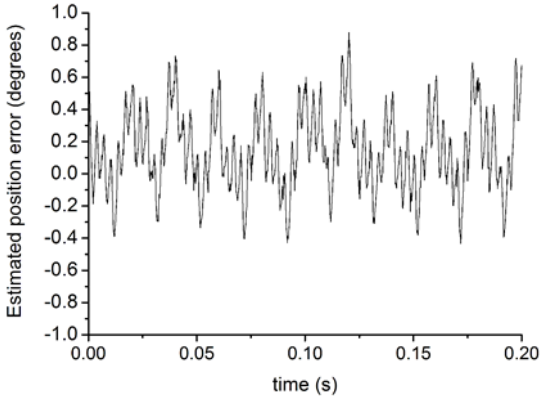

Fig.10 Estimation error at f_b=50Hz (1500rpm) after PWM signal delay compensation

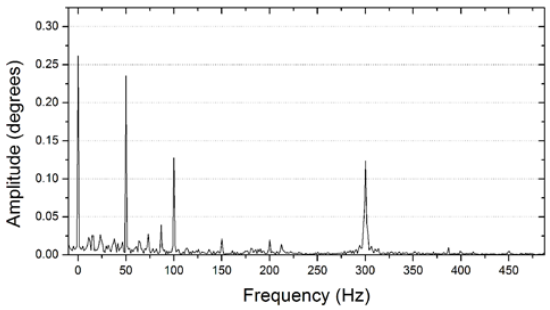

Fig.11 Estimation error and FFT spectrum analysis at f_b=50Hz after PWM signal delay compensation

From Fig. 7, it can be seen that the real voltage u_{real} lags the expected ideal voltage u_{ideal} a short period of time. That is because in "Shadow Mode", the PWM signals will not update until the counter reaches the period or zero value. The delay between ideal voltage and real voltage is half of the PWM cycle time in CTR=PRD shadow mode (Fig.7a) or one PWM cycle time in CTR=Zero shadow mode (Fig.7b). Usually, the phase currents are sampled at the beginning of the PWM cycle, and substituted into the sensorless algorithm, so the calculated position reflects the rotor angle exactly at the beginning moment at each cycle. Then the voltages generated by PI controllers are expected to be output at that moment as well. However, the real output voltages have to be delayed, which makes the rotor response slightly slower than expected. Therefore, the estimated position leads the actual position, and the error is

equal to the angle of the rotor rotated during one delay period. The coefficient *k* in (11) can be detailed as:

$$k = \begin{cases} 0.5 & if\ CTR = PRD \\ 1 & if\ CTR = Zero \end{cases} \quad (12)$$

Compared to those estimation errors contributed by different factors stated above, the PWM signal delay error is the most dominant one. As shown in test results under different speed and PWM frequencies in Fig.8-Fig.9, the position error may reach 7.2 electrical degrees at rated speed (3000rpm, 100Hz) with 5kHz PWM frequency.

Knowing Shadow Mode Register setup, it is possible to compensate this phase-leading DC offset by subtracting it from estimated result:

$$\theta_{est}^{*} = \theta_{est} - \theta_{err\_dc} = \theta_{est} - k \cdot \omega \cdot T_s \quad (13)$$

Fig.8 shows the curve with error compensated. Apparently, the estimation error varies with speed before compensation and could be minimized to less than 1 electrical degree regardless of speed variations.

By subtracting θ_{err_dc} , the component caused by PWM signal delay could be excluded from the estimation error. Fig.10 shows the estimated position error compared to actual position from the encoder, excluding PWM signal delay component, at a fundamental frequency of 50Hz. Fig.11 gives a Fourier spectrum analysis of the error. The error contains components of DC, first, second and sixth harmonics, which are the presents of current measurement error and dead-time effects, as mentioned above.

Conclusions

The estimated position error caused by parameter and variable changes of PMSM vector control system could be concluded as the following aspects:

(1) Resistance variation caused by thermal effect. The error could be safely neglected in wide speed range.

(2) Inductance variation caused by flux saturation. The error is a DC offset at steady state.

(3)Current variation caused by current sensor uncertainties. The error contains DC, first and second harmonics, due to gain error and offset of the sensor measuring.

(4) Voltage loss caused by IGBT dead-time effect. The error contains sixth harmonics, with respect to the dead-time period and the dc-link voltage.

(5) PWM signal delay caused by DSP. The error is a DC offset, with respect to the fundamental frequency and the PWM frequency.

The error caused by PWM signal delay is the most dominant one compared to other aspects, which can be accurately compensated. In addition, the inductance variation is the second significant aspect. In order to get higher estimation accuracy, it is necessary to revise *dq* inductances according to flux saturation in the stator.

The authors acknowledge the Prof. Kaiyuan Lu in Aalborg University, Denmark, equipment support by Smedegaard A/S company, Denmark, the financial support of the National Natural Science Foundation of China (NSFC 51077115) and Zhejiang Provincial Natural Science Foundation of China (R1110033, R1080069).

REFERENCES

[1] F. Genduso, R. Miceli, C. Rando, G. R. Galluzzo, "Back EMF Sensorless-Control Algorithm for High-Dynamic Performance PMSM," IEEE Transactions on Industry Electronics, vol. 57, no. 6, pp.2092-2100, Jun. 2010.

[2]J. Wisniewski, Koczara, W. "The Sensorless Rotor Position identification and Low Speed Operation of the Axial Flux Permanent Magnet Motor Controlled by the Novel PIPCRM Method," Proc. Of PESC'08, Conference Record of the 2008 IEEE, pp. 1502-1507.

[3] M. Hinkkanen, T. Tuovinen, L. Harnefors, J. Luomi, "Analysis and Design of a Position Observer With Stator-Resistance Adaptation for PMSM Drives," International Conference on Electrical Machines (ICEM), 2010, pp. 1-6.

[4] B. N. Mobarakeh, F. M. Tabar, F-M. Sargos, "Back-EMF Estimation Based Sensorless Control of PMSM: Robustness with Respect to Measurement Errors and Inverter Irregularities," 39th IAS Annual Meeting, Conference Record of the 2004 IEEE, vol.3, pp.1858-1865.

[5] A.R. Munoz; T.A. Lipo, "On-Line Dead-Time Compensation Technique for Open-Loop PWM-VSI Drives," IEEE Transactions on Power Electronics, Vol. 14, No. 4, pp. 683-689, July 1999.

[6] Z. Q. Zhu, Y. Li, D. Howe, C. M. Bingham, and D. Stone, "Influence of Machine Topology and Cross-Coupling Magnetic Saturation on Rotor Position Estimation Accuracy in Extended Back-EMF Based Sensorless PM Brushless AC Drives," Proc. of IAS'07, 42nd IAS Annual Meeting, pp.2378-2385.

[7] J. Holtz, J.T. Quan, "Drift and Parameter Compensated Flux Estimator for Persistent Zero Stator Frequency Operation of Sensorless Controlled Induction Motors," IEEE Transactions on Industry Applications, vol. 39, no. 4, pp. 1052-1060, Jul./Aug. 2003.

[8] S. Shinnaka, K. Sano, "A New Unified Analysis of Estimate Errors by Model-Matching Phase-Estimation Methods for Sensorless Drive of Permanent Magnet Synchronous Motors and New Trajectory-Oriented Vector Control," Electrical Engineering in Japan, Vol. 168, No. 1, 2009, pp. 52-65.

[9] T.H. Kim, M. Ehsani, "An Error Analysis of the Sensorless Position Estimation for BLDC Motors," 38th IAS Annual Meeting. Conference Record of the 2003 IEEE, vol.1, pp.611-617.

[10] J. Arellano-Padilla, C. Gerada, G. Asher, M. Sumner, "Inductance Characteristics of PMSMs and their Impact on Saliency-based Sensorless Control," 14th International Conference of Power Electronics and Motion Control, EPE-PEMC 2010, pp. S1-1-S1-9.

[11] C. Silva, G.M. Asher, M. Sumner, "Influence of Dead-time Compensation on Rotor Position Estimation in Surface Mounted PM Machines using HF Voltage Injection," Proc. of the Power Conversion Conference 2002, pp.1279-1284.

[12] J. Holtz, "Acquisition of Position Error and Magnet Polarity for Sensorless Control of PM Synchronous Machines," IEEE Transactions on Industry Applications, vol. 44, no. 4, Jul./Aug. 2008.

[13] Texas Instruments Incorporated, "TMS320x2833x, 2823x Enhanced Pulse Width Modulator (ePWM) Module," Literature Number: SPRUG04A, Oct. 2008–Jul. 2009.

Authors

Associate professor Qinfen Lu works in college of Electrical Engineering, Zhejing Unversity, P.R.China, 310027, Email: luqinfen@zju.edu.cn.